Nighttime air quality under desert conditions

Wendy S. Goliff[1], Menachem Luria[2], Donald R. Blake[3], Barbara Zielinska[4], Gannet Hallar[4], Ralph J. Valente[5], Charlene V. Lawson[6,7], William R. Stockwell[4,6]

[1]College of Engineering Center for Environmental Research and Technology University of California, Riverside
[2]The Hebrew University in Jerusalem, Earth Science Institute
[3]Department of Chemistry, University of California, Irvine
[4]Division of Atmospheric Sciences, Desert Research Institute, Reno, Nevada
[5]Environmental Technologies Department, Tennessee Valley Authority, Muscle Shoals, Alabama, USA.
[6]Howard University, Department of Chemistry, Washington, DC
[7]Environmental Sciences, Shell Global Solutions (US), Houston, Texas

Corresponding Author: Wendy S. Goliff, College of Engineering Center for Environmental Research and Technology University of California, Riverside, 1084 Columbia Avenue, Riverside, CA 92507, phone: 951 781-5665; fax: 951-781-5790; email: wendyg@cert.ucr.edu

Key words: Nighttime chemistry; nitrate radical; free troposphere; 0-D modeling; tropospheric measurements

Abstract

Nighttime concentrations of the gas phase nitrate radical (NO_3) were successfully measured during a four week field campaign in an arid urban location, Reno Nevada, using long-path Differential Optical Absorbance Spectrometry (DOAS). While typical concentrations of NO_3 ranged from 5 to 20 ppt, elevated concentrations were observed during a wildfire event. Horizontal mixing in the free troposphere was considerable because the sampling site was above the stable nocturnal boundary layer every night and this justified a box modeling approach. Process analysis of box model simulations showed NO_3 accounted for approximately half of the loss of internal olefins, 60% of the isoprene loss, and 85% of the α-pinene loss during the nighttime hours during a typical night of the field study. The NO_3 + aldehyde reactions were not as important as anticipated. On a polluted night impacted by wildfires upwind of the sampling location, NO_3 reactions were more important. Model simulations overpredicted NO_2 concentrations for both case studies and inorganic chemistry was the biggest influence on NO_3 concentrations and on nitric acid formation. The overprediction may be due to additional NO_2 loss processes that were not included in the box model, as deposition and N_2O_5 uptake had no significant effect on NO_2 levels.

1. Introduction

Nitrogen oxides (NO_x = nitric oxide (NO) + nitrogen dioxide (NO_2)) are important precursors for the formation of tropospheric ozone and nitrate containing aerosols (Frost et al. 2006; Ng et al. 2007). These are produced through a highly non-linear mechanism involving nitrogen oxides and volatile organic compounds (VOC).

Multi-day regional scale modeling studies were among the first to show that nighttime losses of NO_x could affect ozone formation on subsequent days (e.g., Dimitroulopoulou and Marsh 1997). Many of the known nighttime loss mechanisms for NO_x involve the formation of the nitrate radical (NO_3).

Nitrate radical is formed in the troposphere by the reaction of NO_2 with O_3 (Atkinson et al. 2006).

$$NO_2 + O_3 \rightarrow NO_3 + O_2;\ k_1\ (298K) = 3.5 \times 10^{-17}\ cm^3\ s^{-1} \quad (1)$$

The formation of NO_3 results in only small NO_x losses during the day because NO_3 rapidly photolyzes to regenerate NO and NO_2 under unobstructed clear sky conditions. The concentration of NO_3 is very low in the presence of appreciable NO during the day and nighttime due to Reaction 2.

$$NO_3 + NO \rightarrow 2NO_2 \quad (2)$$

NO_3 may also undergo thermal decomposition:

$$NO_3 + M \rightarrow NO + O_2 + M \quad (3)$$

However, this reaction is slow ($2.5 \times 10^6 \exp(-6.1 \times 10^3/T)\ s^{-1}$; Johnston et al. 1986).

During the nighttime in regions with low NO concentrations NO_3 reacts with a number of VOC to produce nitric acid (HNO_3) that in the presence of gas-phase ammonia (NH_3) can react to produce ammonium nitrate (NH_4NO_3). Under the proper conditions of humidity and temperature NH_4NO_3 will exist as a solid phase aerosol (Stelson and Seinfeld 1982). For example, NO_3 abstracts H atoms from

saturated hydrocarbons to form HNO_3 but these reactions are slow, on the order of 10^{-17} cm^3 $molecule^{-1}$ s^{-1}. More important in the polluted atmosphere is the reaction of NO_3 with aldehydes to form HNO_3, hydroperoxy radical (HO_2) and organic peroxy radicals (RO_2) (Stockwell and Calvert 1983; Cantrell et al. 1985). NO_3 reacts with alkenes by its addition to double bonds with k_{298} in the range of 10^{-16} to 10^{-11} cm^3 $molecule^{-1}$ s^{-1}). The nighttime reactions of NO_3 with alkenes can be a loss mechanism for alkenes that is as important as their daytime reactions with HO (Geyer et al. 2003; Brown et al. 2011).

Important indirect sinks for NO_3 involve the formation of dinitrogen pentoxide (N_2O_5).

$$NO_2 + NO_3 + M \leftrightarrow N_2O_5 + M \qquad (4)$$

Although Reaction 5 is slow in the gas phase due to entropy considerations (Calvert and Stockwell 1983, Wahner et al. 1998):

$$N_2O_5(g) + H_2O(g) \rightarrow 2HNO_3(g) \qquad (5)$$

Reaction 6 is fast on aerosols coated with liquid water (Chang et al. 2011).

$$N_2O_5(g) + H_2O(aq) \rightarrow 2HNO_3(aq) \qquad (6)i$$

Previous field measurements of NO_3 include Geyer et al. (2001; 2003) in which measurements of significant daytime mixing ratios of nitrate radical were as high as 30 ppt beginning at 3 hours before sunset. Brown et al. (2005) conducted measurements of NO_3 during the day with values of 0.5 pptv recorded, which is highly reactive with α-pinene, indicating that it can account for 10-40% of its oxidation. Sommariva et al. (2009) conducted measurements on the NOAA research vessel ***Ron Brown***, and found that modeled NO_3 was overestimated by 30-50% in the marine boundary layer at night and called for more studies of peroxy radicals and NO_3 as a potential nighttime loss of NO_3. Salisbury et al. (2001) conducted measurements of HO_2+RO_2, NO_3 with DOAS, HCs and ozone at a coastal site in Ireland. They found the most important reactions at night with respect to radical production were O_3 and NO_3 reactions. NO_3 reactions dominated in cleaner marine air from the West, and found that NO_3 is both a source and sink of RO_2.

Emerson and Carslaw (2009) performed a measurement campaign in rural area of the UK, 25 miles from London. Simultaneous measurements were made of meteorological conditions, aerosol size distribution and composition, concentrations of HO, HO_2, HO_2 + ΣRO_2, non-methane hydrocarbons (NMHC), oxidized VOCs), CO, NO, NO_2, H_2O, and O_3. Although they did not measure NO_3, they applied the Master Chemical Mechanism (MCM; Jenkin et al. 1997; 2003) to simulate it and found a nighttime average NO_3 concentration of 0.6 ppt for their conditions. Their model simulations estimated that NO_3 initiated the formation of 33% of RO_2 species.

Asaf et al. (2009) measured NO_3 in an urban location for two years. The average nighttime concentration maximum was 200 ppt with maximum levels exceeding 800 ppt. Their measurements showed NO_3 was inversely correlated with relative humidity and positively correlated with temperature and to a lesser extent with NO_2 and O_3, indicating that heterogeneous removal processes were also important.

Benton et al. (2010) measured the sum of NO_3 + N_2O_5 with a broadband cavity enhanced absorption spectroscopy system (BBCEAS) located 160m above street level in London. They found that NO_3

concentrations were not likely to reach steady state during their campaign. Calculated lifetimes of NO_3 were on the order of a few minutes. Crowley et al. (2010) measured NO, NO_2, NO_3 and N_2O_5 at a rural mountain site in Germany. In remote areas, the lifetime of NO_3 is controlled by reactions with VOCs. NO_3 and N_2O_5 were measured using an off-axis cavity-ring-down system (OA-CRD).

Crowley et al. (2011) measured NO_3 and N_2O_5 with OA-CRD on the Atlantic Coast of southern Spain in a forested area near both pollution sources and the Atlantic Ocean. NO_3 lifetimes were longest in air masses originating over the Atlantic Ocean, and were very short (a few seconds) in polluted air masses.

Stone et al. (2014) measured NO_3, N_2O_5, HO and HO_2 in an aircraft over the UK and the North Sea to assess the importance of nighttime chemistry on regional and global air quality. They attempted to interpret their observations using a zero-dimensional model using the Master Chemical Mechanism v3.2. They found that their model systematically underpredicted HO_2 by approximately 200% and overpredicted NO_3 and N_2O_5 by around 80 and 50%, respectively.

These observations suggest that much more remains to be learned about production and loss processes for the nitrate radical. (Readers are directed to the excellent review article by Brown and Stutz (2012) for a more in depth look at nocturnal chemistry.) In this project our objective is to evaluate the impact of nitrate radical on the transformation and removal of atmospheric compounds under conditions of low relative humidity. This project provides the first continuous measurements of nitrate radical over a period of four weeks in an arid urban location, Reno, Nevada, USA.

2. Site Description

This study was performed at the Desert Research Institute (DRI) located at 39.52°N 119.81°W, 1509 m ASL) on a mesa to the north of Reno (about 400 meters from Highway US Route 395) during July and August of 2008. Reno is an urban area (population ca. 200,000) in a semi-arid valley between the Sierra Nevada and Virginia mountain ranges. Reno is bordered to the east by the city of Sparks. The Reno-Sparks metropolitan area is informally called the Truckee Meadows, and consists of about 400,000 residents. Due to the effect of the Sierra Nevada mountain range on wind flow patterns, pollutant concentrations in Reno, NV are mostly local in origin although some long-range transport from the San Francisco Bay Area and central California may occur.

The air quality in Reno is moderately polluted with peak ozone mixing ratios typically between 60 to about 95 ppb, peak NO_x levels on the order of 50 to 80 ppb and there are frequent episodes of high particulate concentrations (Stanley et al., 1997; Washoe County, 2014). These levels of O_3 suggest that NO_3 is not likely to reach detectable levels during the daytime because Geyer et al. 2003a required O_3 mixing ratios exceeding ~100 ppb for nitrate radical to reach detectable levels. However, Reno is in a relatively deep valley with considerable shading (attenuating solar radiation) that reduces NO_3 photolysis during the late afternoon.

The relative humidity in Reno, NV is low enough for hydrolysis to be slow, leading to concentrations of nitrate radical high enough to be observed. The average relative humidity is 26, 18 and 35% at 10:00, 16:00 and 22:00, respectively, during July for the previous ten years (Western Regional Climate Center: www.wrcc.dri.edu). However, during this campaign (July 2008), relative humidities were even lower: 11,

9 and 14% at 10:00, 16:00 and 22:00, respectively. Givens the presence of high ozone, NO_x and low relative humidity, the mixing ratios of nitrate radical were easily observed during the nighttime hours.

3.0 Methods

3.1 Measurements

Measurements were conducted nightly for VOCs and NO_3 from 7 July 2008 to 8 August 2008. Long-path Differential Optical Absorbance Spectrometry (DOAS) is an established procedure for measuring gaseous constituents of the atmosphere, and is based on ultraviolet-visible absorption spectroscopy. A DOAS instrument has three necessary components: a source of broadband light, a focused light path long enough for significant absorbance by the constituent gases (e.g., a combination of telescope and reflectors) and a detector capable of measuring light intensity over a range of wavelengths (e.g., a multichannel spectrometer). What distinguishes DOAS from other forms of absorption spectroscopy is that it's a single-beam technique with the reference beam intensity estimated from an interpolated background. The DOAS instrument was used to measure the concentrations of the atmospheric species, NO_3, NO_2, O_3, CO, SO_2 and HCHO.

For this project, the DOAS was obtained on loan from the Air Quality Laboratory at the Institute of Earth Sciences, Hebrew University of Jerusalem. The system was manufactured by Hoffmann-Messtechnik, Rauenberg, Germany, and consists of a transmitting/receiving telescope housing, containing a light source and connected to a diffraction-grating spectrometer with a 1024 channel photodiode array detector. The DOAS system was mounted on the top floor of DRI's Northern Nevada Science Center (NNSC) building on the outskirts of the urban area. The light path was directed toward the south of DRI to a set of retro-reflectors mounted on the rooftop of the Grand Sierra Resort in downtown Reno, a distance of 5.86 kilometers each way, Figure 1. (For detection limits of this and other instruments used in this study see Table 1.)

The field study provided four weeks of continuous measurements of nitrate radical, meteorological variables, particulate nitrate and sulfate, and ancillary species during the summer along with 30-minute integrated samples of hydrocarbons and aldehydes which were collected once or twice per day throughout the intensive, Tables 1 and 2. A wide range of relative humidities were expected due to the low absolute water vapor concentrations and the relatively strong diurnal temperature variations that occur in desert environments during the summer. Another major possibility that could affect the nitrate radical concentrations was wildfires that often occur and can significantly increase the concentrations of aerosol particles for weeks at a time. Some of the measurements were in fact made during wildfires that affected the Reno area.

Temperature, solar radiation, relative humidity, wind speed and direction, and barometric pressure were monitored continuously from sunset until sunrise along with mixing ratios of NO, NO_2, O_3, total nitrogen oxides, CO, CO_2, and SO_2 which were measured by real time analyzers using chemiluminescence or optical absorbance instrumentation from the Tennessee Valley Authority. Particulates were measured nightly by a Scanning Mobility Particle Sizer (SMPS™) spectrometer for submicrometer particle sizing (obtained on loan from the Storm Peak Laboratory, Steam Boat Springs, CO for this project).

Canister samples were collected for analysis volatile organic compounds on the rooftop of DRI, Table 1. These samples were then sent to the University of California, Irvine laboratory for analysis using three gas chromatography (GC) ovens coupled with a suite of detectors that together are sensitive to 76 C_2–C_{10} VOCs, using two flame ionization detectors (FIDs) to measure hydrocarbons, two electron capture detectors (ECDs) for halocarbons, and a quadrupole mass spectrometer detector (MSD) for sulfur compounds (Simpson et al. 2010). DNPH (2,4-dinitrophenylhydrazine) cartridge samples of aldehydes were collected using the EPA TO-11A method were made during the intensive, which were analyzed by the Organic Analytical Laboratory at DRI (see Table 1 for instrument description).

The time resolution for each instrument ranges from 5 to 15 minutes (all continuous meteorological measurements to 15 minutes DOAS measurements) and the recorded measurements were synchronized. VOC samples (canisters and DNPH cartridges) were also synchronized to cover the two fifteen-minute sampling intervals of the DOAS. It is evident that the DOAS is not a point measurement. However, the optical path was located so that the impact by local sources would be minimized. We believe the increased sensitivity of this measurement outweighed any uncertainties due to differences in spatial resolution. Furthermore, the differences in measurements of ozone and NO_2 between the point samples and the DOAS were less than 10%, therefore local effects were not observed.

The DOAS spectra were analyzed following well-established procedures for the identification and quantification of atmospheric gaseous species (e.g., Heintz et al. 1996; Geyer et al. 1999). Background spectra, dark current, and electronic offset were subtracted, followed by band-pass filtration of the resulting spectra. A fifth order polynomial and reference spectra for NO_2 (measured on site), NO_3 (literature values), and water vapor (from daytime spectra with no NO_3 present) were fitted using nonlinear least-squares fitting routines by the analysis software MFC (Asaf et al. 2009).

The measurements of the NO_3 concentrations and of the ancillary species were analyzed in order to evaluate their sources, chemical processes, oxidative capacity, sinks, and products. The important parameters governing the NO_3 chemistry can be calculated from the ancillary data, including nitrate radical production rates, NO_3 lifetime, concentrations of N_2O_5 (which is in equilibrium with nitrate radical and may serve as a major sink under some conditions), oxidation capacity, nitrate radical degradation frequency, and direct and indirect removal rates. The measured ancillary species were used to estimate the expected gas-phase losses of nitrate radical through reactions with VOC and NO_x.

Additional meteorological information was obtained using a miniSODAR (Atmospheric Systems Corporation, Santa Clarita, CA), which can measure the winds in the range of 30 to 200 meters above the ground in 5 meter increments; and a Vaisala Ceilometer CL-31, which measures vertical visibility with infrared light (λ=910 nm) to establish boundary layer heights as a function of time. The miniSODAR was located in the parking lot of DRI, while the ceilometer was located on the rooftop of DRI.

3.2 Modeling

The RACM2 mechanism (Goliff et al. 2013) was employed in a box model (SBOX: Seefeld 1997) to simulate ambient field data collected during the summer 2008 campaign. RACM2 uses a lumped molecular approach for representing atmospheric chemistry. It consists of 363 chemical reactions including 33 photolytic reactions and uses 120 chemical species to describe atmospheric chemistry. It uses kinetic data from several sources including the recent suggestions of IUPAC (IUPAC 2010) and

NASA/JPL (Sander et al. 2011). It was evaluated by comparing simulation results with environmental chamber experimental data from the University of California, Riverside and the EXACT campaign (Goliff et al., 2013). For daytime simulations, photolysis frequencies were calculated from the absorption cross-sections and quantum yields referenced in (Goliff et al. 2013) and spectrally resolved actinic flux calculated according to Madronich (1987).

The box model SBOX using RACM2 was run with and without dry deposition for the following compounds: O_3, NO_2, N_2O_5, HNO_3 and PAN. Deposition rates were taken from Pugh et al. 2010 (ozone, NO_2 and HNO_3); Rohrer et al. 1998 (N_2O_5); and Schrimpf et al. 1996 (PAN). The model was constrained by observations of organic and inorganic compounds measured during the campaign. For the two case studies presented in this manuscript, initial conditions were taken from observations at the beginning of the night. Radical intermediates reach a steady state based on the initial concentrations within a few simulated seconds during a chemical box model simulation. No spin-up time is required because of the very rapid establishment of a steady state of the reactive intermediates and the box model assumption of instantaneous perfect mixing.

4. Results and Discussion

4.1 Measurements

Concentrations of NO_3 were measured above the detection limit every night with the exception of portions of the nights of July 9-10, July 10-11, and July 12-13, 2008 (on the night of July 11-12 the wind shifted to the East). These nights were impacted by wildfires upwind in northern California. Severe light scattering from the fire-generated particles prevented the DOAS from making nitrate radical measurements during most of these three nights. During these nights there was elevated particulate matter, CO, VOCs and NO_2. The highest nighttime ozone observed throughout the field campaign was on the night of July 9-10, when ozone peaked at 88 ppb. Carbon monoxide, acetone and many measured aldehydes were elevated on these high O_3 nights compared to the rest of the field campaign (Figure 2a-c).

The sampling location on the rooftop of DRI was in the free troposphere for much of the night throughout the campaign. This conclusion is supported by CO measurements conducted during the campaign. Figure 3 illustrates the CO and ozone concentrations for the night of July 13-14, 2008, in which spikes in the CO concentrations (the result of mobile emissions from the valley floor) are observed at 6 a.m. and 8 a.m. local time. We believe the first spike is due to updrafts of air due to warming of the hillside, and the second spike is due to the boundary layer height rising to the height of the sampling location. These pairs of CO spikes were observed every morning of the field campaign. In addition to the CO spikes, we observed concurrent dips in the ozone concentrations due to the titration of ozone by NO (also from mobile emissions).

Figure 4 shows the nocturnal half-hourly mixing ratios of NO_3 measured by the DOAS during the entire measurement campaign. Higher concentrations were generally observed during the second half of the night, with levels dropping at dawn, which was approximately 5:30 a.m. local time. Table 3 shows the range and average nighttime concentrations for NO, NO_2, NO_3, O_3 and CO for the entire campaign. The highest concentrations of nighttime NO_3 and O_3 were observed on the nights when Reno air quality was influenced by wildfires in northern California. The highest NO_2 values were observed during the hours of the early morning commute due to the presence of nearby US Route 395.

The measured NO_3 concentrations were not sensitive to relative humidity, the concentrations of NO_2 or ozone during the entire campaign as shown by their lack of correlations in the data. However, NO_3 did correlate with NO, implying that NO concentrations were the main driver for NO_3 destruction for the Reno conditions. Nighttime NO concentrations ranged from 0.004 to 3.86 ppb throughout the campaign, with an average of 0.7 ppb. Possible local sources were soil and vehicle traffic from nearby highway US Route 395. As expected, NO concentrations inversely correlated with ozone concentrations**.**

Concentrations of total particle numbers were highest while Reno, Nevada was downwind of the wildfire event the nights of July 9-10, July 10-11, and July 12-13, 2008, peaking at 12000 particles per cubic centimeter. Particle concentrations on typical nights in Reno were in the vicinity of 2500 particles per cubic centimeter. Figure 5(a) shows the observed particle diameters for a night impacted by the fires, and Figure 5(b) shows particle diameters on a typical night. While the particles on a typical night show a bimodal distribution of diameters, this is not case for the night downwind of the California fires, during which the diameters are larger, peaking at around 200 nm.

4.2.1 Comparing model output to observations

In this manuscript we present the results of box model simulations for two nights in Reno, NV: July 30-31, 2008 (a typical night in Reno) and July 10-11 (a night impacted by wildfires from California). The difference between these nights is illustrated in Figure 6. On July 10-11 ozone and NO_2 was higher for the first half of the night than July 30-31. NO was lower by about 50% the night of July 10-11 for the entire night. NO_3 measurements were sporadic for the first half of the night of July 10-11 due to high particle concentrations from the California wildfires interfering with the light path of the DOAS. For the second half of both nights, NO_3 concentrations were slightly higher on July 30-31, 2008. The temperature and relative humidity for both nights were essentially the same.

Case Study #1: the night of July 30-31, 2008 - a typical night in Reno, NV

During the night of July 30-31, 2008 in Reno, NV, ozone levels were approximately 50 ppb throughout the night, NO was 0.8 ppb, NO_2 averaged 3 ppb, and NO_3 was measured to be 5 ppt. The measured VOC/NOx ratio was 15 at 8:25 p.m. July 30 and 8 at 5:20 a.m. July 31. The box model was able to reproduce the ozone, NO, and NO_3 levels (which were underestimated during the second half of the night), but not the NO_2 concentrations. In fact, the model overestimated NO_2 concentrations by factor of 3 during the night. Even when dry deposition is accounted for, model output for NO_2 continues to be overestimated. There are several possible reasons for this. One is that the box model has greater mixing than what is realistic for nighttime conditions, even in the free troposphere. This explanation seems unlikely due to the fact that the DOAS measurements and point measurements are in good agreement. Another possible reason may be due to N_2O_5 uptake by aerosols. (Uptake efficiencies tend to be higher for N_2O_5 than NO_3, so we will limit our discussion to N_2O_5 (Chang et al., 2011)). Therefore we added N_2O_5 uptake by aerosols to the model, using an uptake coefficient of 0.002 due to the low humidity. The model predicted N_2O_5 concentrations lowered by 1 ppt for the night of July 30-31 and lowered by 0.5 ppt on the night of July 10-11. Although there is a higher surface area density on the night of July 10-11, the aerosol is due to biomass burning, which contains a higher percentage of organic carbon (Singh et al. 2010), which has been shown to impede N_2O_5 uptake (Chang et al., 2011). Another possibility is that there is an additional, unaccounted for, removal mechanism for NO_2.

Case Study #2: the night of July 10-11, 2008, Impact of wildfires from California in Reno, NV

During the night of July 10-11, 2008, the measured VOC/NOx ratio was 108 at 11 p.m. on July 10 and 79 at 3a.m. July 11. The box model was able to replicate the ozone levels, underestimate NO concentrations by about 15%, underestimate NO_3 levels by an average of 50%, and overestimate NO_2 concentrations by 50% at the beginning of the night a factor of 2.5 during the second half of the night. Adding dry deposition to the model did little to change those numbers (<5%). The model was less able to simulate observed values for these compounds possibly because the VOC/NO_x ratio was much higher than is typically observed in urban areas. VOC/NO_x ratios in the vicinity of 100 are typically found in remote areas where NO concentrations are very low. For this case study, NO is not low, rather VOC concentrations were very high due to the influence of the California wildfires.

4.2.2 Process Analysis

In many cases a steady state assumption for NO_3 concentrations (defined as when the production and loss rates are equal and the concentration of the species is unchanged) is not valid due to the presence of N_2O_5 as a reservoir species which is in equilibrium with NO_3 and NO_2 (reaction 4) and the possibility of N_2O_5 removal by hydrolysis, aerosol uptake and deposition. For the conditions present in this study, the warmer temperatures and low NO_2 concentrations allow for the system to reach steady state faster than most other scenarios (Brown et al., 2003), particularly when removal rates for N_2O_5 are slow (detailed below).

July 30-31, 2008

Reaction with NO_3 was a significant loss process for the model species OLI (olefins with an internal double bond), DIEN (olefins with two double bonds), ISO (isoprene), and API (α-pinene). Table 4 illustrates the relative importance of NO_3 reactions compared to HO and O_3 reactions. NO_3 reactions accounted for slightly more than half of the loss (60%) of OLI, less than half of the loss (28%) of DIEN, 60% of the loss for ISO, and 85% of API for most of the night. NO_3 contributions for aldehyde degradation were much smaller, generally less than 10%, and 20% for OLT (olefins with a terminal double bond).

July 10-11, 2008

Table 4 shows the relative loss rates for the model species OLI, DIEN, ISO and API for July 10-11, 2008. In the case of every model species, NO_3 reactions are more important on July 10-11 than on July 30-31. This is likely because the model predicts lower HO concentrations of 7.6×10^{-6} ppb on July 10-11 (Figure 7 ~~9~~) during the second half of the night compared to 3.6×10^{-5} ppb on July 30-31. Figure 8 shows the predicted HO_2 concentrations for each case study. While July 10-11 had lower HO concentrations than July 30-31, HO_2 concentrations were higher: peak value of 4.7×10^{-3} ppb HO_2 on July 10-11 and 1.2×10^{-3} ppb HO_2 on July 30-31. This may be because CO and formaldehyde (HCHO) were elevated on July 10-11 (1318 ppbv CO and 27 ppbv HCHO on July 10-11 and 152 ppbv CO and 4.7 ppbv HCHO on July 30-31), and served to convert HO to HO_2 during the night.

Case Study Comparisons

Figure 9 illustrates which reactions are most important for overall HO_x ($HO + HO_2$) formation during the nighttime hours on July 10-11 and July 30-31, 2008. For both nights, the OLI + O_3 and OLT + O_3 reactions are most important, ranging from 68% - 80% of the total HOx formation. The ISO + O_3 reaction is more important on the night of July 10-11 (with an average of 12% contribution to HOx) than the night of July 30-31 (with an average of 4% contribution), which was expected due to isoprene concentrations being 2 times greater on the night of July 10-11. The model species DCB1, DCB2 and EPX are products of the oxidation reactions of aromatic compounds and they react with ozone to form HO and/or HO_2 in RACM2.

The calculated HO_2/HO ratios were quite different for each case study: an average of 101 on July 30-31 and 185 on July 10-11 (Figure 10), even though the measured NO was lower on July 10-11; however, that night had elevated concentrations of HCHO and CO which also serve to convert HO to HO_2. Elshorbany et al. (2012) state that a high HO_2/HO ratio is typical for clean air with low NOx conditions. The model calculations in this study show a high HO_2/HO ratio may also be seen with polluted air with low NO (NO $\approx$1 ppb) conditions as well.

While the most important removal mechanism during the nighttime hours for NO_3 is reaction with NO, the removal of NO_3 by hydrocarbons varied with the two case studies discussed in this paper. Figure 11 shows OLT + NO_3 (average of 6%) OLI + NO_3 (average of 41%) and ISO + NO_3 (average of 42%) as important for NO_3 removal by hydrocarbons on both nights, although OLI is more dominant for much of the night on July 30-31 than on July 10-11 (average of 67%).

Process analysis was also employed to investigate the importance of various reactions with regard to nitric acid (HNO_3) formation. For both case studies, the most important reaction was NO_2 + HO. For the night of July 10-11, when VOC concentrations were elevated due to the wildfires in California, NO_2 + HO accounted for 40% of nitric acid formation at the beginning of the night, and 80% at the end of the night (Figure 12), with the remainder due to oxygenated VOCs + NO_3 and other inorganic reactions. On July 30-31, NO_2 + HO accounted for 86% of the nitric acid formation for most of the night (Figure 12). Acetaldehyde (ACD in RACM2) was the most important contributor to nitric acid formation among the oxygenated VOCs reacting with NO_3 (10%).

Because the model overpredicts NO_2, we adjusted the model parameters to force a fit to observed NO_2 concentrations. Under these conditions, the NO_2 + HO reaction accounted for 76% of nitric acid formation for most of the night of July 30-31, while the impact of this reaction remained unchanged for the night of July 10-11, and remains the most important HNO_3 formation reaction in these case studies. An additional consequence of the model adjustment, the hydroxyl radical concentrations dropped 4% for the night of July 30-31 and 0.4 % for the night of July 10-11.

5. Conclusions

Nighttime concentrations of nitrate radical were successfully measured during a four week field campaign in an arid urban location, Reno Nevada. While typical concentrations of NO_3 ranged from 5 to 20 ppt, elevated concentrations were observed during a wildfire event. On a typical night in Reno, Nevada, NO_3 accounted for approximately half of the loss of olefins, 60% of the isoprene loss, and 85% of the α-pinene loss during the nighttime hours. The NO_3 + aldehyde reactions were not as important as anticipated. On a polluted night with elevated VOCs. For both case studies discussed here, inorganic chemistry was the

biggest influence on NO_3 concentrations and on nitric acid formation. Model simulations overpredicted NO_2 concentrations for both case studies. This may be due to NO_2 removal processes that were not accounted for. It's also possible that the box model may have greater than realistic mixing then suitable for simulating the measurement period. However, the sampling location was in the free troposphere, above the boundary layer every night, so it's unlikely that the air was stagnant. Future studies include box modeling with dilution terms simulating horizontal dispersion, examination of the impact of different chemical mechanisms on model simulations and analysis of the effects of mountain meteorology with a 1-D model to further explore the impact of mixing on NO_2 and CO concentrations, as well as vertical flux and deposition.

Acknowledgements

The authors gratefully acknowledge the Facilities Department at the Desert Research Institute for remodeling the Science Tower specifically for the purposes of conducting the field campaign discussed in this manuscript. We also thank Dr. Ming Xiao for assistance with the SMPS data, Dr. David DuBois for assistance with the ceilometer data, and Ms. Michelle Breckner for her assistance with the miniSODAR at Desert Research Institute. NSF provided funding through NSF Award Number: 0701221 for this project and the NSF Research Experiences for Undergraduates program to the Desert Research Institute. NSF provided funding through NSF Award Number: 0653997 for this project. The authors thank the National Oceanic and Atmospheric Administration for a grant to Howard University's NOAA Center for Atmospheric Sciences and the National Aeronautics and Space Administration for a grant to "Howard University Beltsville Center for Climate System Observation," these grants helped support the data analysis. The authors thank Howard University graduate student Tatiana D. Gonzalez for helpful discussions. The authors also thank University of Nevada Reno undergraduate student Ramona Hull for assistance in running the SBOX model for the case studies. The opinions expressed in this publication are those of the authors alone and do not reflect the policy of any government agency.

References

Asaf D., Pedersen D., Matveev V., Peleg M., Kern C., Zingler J., Platt U., and Luria M., 2009: Long-Term Measurements of NO_3 Radical at a Semiarid Urban Site: 1. Extreme Concentration Events and Their Oxidation Capacity, *Environ. Sci. Technol*. **43** (24), 9117-9123.

Atkinson et al. 2006: http://www.iupac-kinetic.ch.cam.ac.uk/

Brown, S. S., H. Stark, and A. R. Ravishankara, Applicability of the steady state approximation to the interpretation of atmospheric observations of NO_3 and N_2O_5, J. Geophys. Res., 108(D17), 4539, doi:10.1029/2003JD003407, 2003.

Brown, S.S., Dubé, W.P., Peischl, J., Ryerson, T.B., Atlas, E., Warneke, C., de Gouw, J.A., te Lintel Hekkert, S., Brock, C.A., Flocke, F., Trainer, M., Parrish, D.D., Feshenfeld, F.C., Ravishankara, A.R., 2011: Budgets for nocturnal VOC oxidation by nitrate radicals aloft during the 2006 Texas Air Quality Study, *J. Geophys. Res*. **116**, D24305. doi:10.1029/2011JD016544

Brown, S. S., & Stutz, J. (2012). Nighttime radical observations and chemistry. *Chemical Society Reviews*, 41(19), 6405-6447.

Calvert J. G. and Stockwell W. R., 1983: Acid generation in the troposphere by gas-phase chemistry, *Environ. Sci. Technol.* **17** (9), pp 428A–443A DOI: 10.1021/es00115a727

Cantrell, Christopher A., Stockwell, William R., Anderson, Larry G., Busarow, Kerry L., Perner, Dieter, Schmeltekopf, Art, Calvert, Jack G., and Johnston, Harold S., 1985: Kinetic study of the nitrate free radical (NO_3)-formaldehyde reaction and its possible role in nighttime tropospheric chemistry, *J. Phys. Chem.* **89** (1), 139-146.

Chang, W. L., Bhave, P. V., Brown, S. S., Riemer, N., Stutz, J., Dabdub, D., 2011: Heterogeneous atmospheric chemistry, ambient measurements, and model calculations of N_2O_5. A review, *Aerosol Sci. Technol.* **45**, 665–695, doi:10.1080/02786826.2010.551672.

Dimitroulopoulou, C., Marsh, A.R.W., 1997: Modelling studies of NO_3 nighttime chemistry and its effects on subsequent ozone formation, *Atmos. Environ.* **31**(18), Pages 3041-3057. (http://www.sciencedirect.com/science/article/pii/S1352231097000332)

Elshorbany, Y. F., et al., 2012: HOx budgets during HOxComp: A case study of HOx chemistry under NOx-limited conditions, *J. Geophys. Res.* **117**, D03307, doi:10.1029/2011JD017008.

Frost, G. J., et al., 2006: Effects of changing power plant NOx emissions on ozone in the eastern United States: Proof of concept, *J. Geophys. Res.* **111**, D12306, doi:10.1029/2005JD006354.

Geyer, A., B. Alicke, S. Konrad, J. Stutz, and U. Platt, 2001: Chemistry and oxidation capacity of the nitrate radical in the continental boundary layer near Berlin, *J. Geophys. Res.*, **106**, 8013–8025.

Geyer, A., Bachmann, K., Hofzumahaus, A., Holland, F., Konrad, S., Klupfel, T., Patz, H.-W., Perner, D., Mihelcic, D., Schafer, H.-J., Volz-Thomas, A., Platt, U., 2003: Nighttime formation of peroxy and hydroxyl radicals during the BERLIOZ campaign: Observations and modeling studies, *J. Geophys. Res.* **108**, 8249, doi:10.1029/2001JD000656.

Goliff, Wendy S., Stockwell William R., Lawson Charlene V., 2013: The regional atmospheric chemistry mechanism, version 2, *Atmos. Environ.* **68**, 174-185, ISSN 1352-2310, 10.1016/j.atmosenv.2012.11.038.

IUPAC 2010: http://www.iupac-kinetic.ch.cam.ac.uk/

Jenkin, M.E., S.M. Saunders, and M.J. Pilling, 1997: The tropospheric degradation of volatile organic compounds: A protocol for mechanism development, *Atmos. Environ.* **31**, 81-104.

Jenkin, M.E., S.M. Saunders, V. Wagner, and M.J. Pilling, 2003: Protocol for the development of the Master Chemical Mechanism, MCM v3 (Part B): tropospheric degradation of aromatic volatile organic compounds, *Atmos. Chem. Phys.* **3**, 181–193.

Johnston, H. S., Cantrell, C. A., Calvert, J. G., 1986: Unimolecular Decomposition of NO_3 to Form NO and O_2 and A Review of N_2O_5/NO_3 Kinetics, *J. Geophys. Res.* **91**(D4), 5159–5172, doi:10.1029/JD091iD04p05159.

Madronich, S.. 1987: Photodissociation in the Atmosphere; 1. Actinic Flux and the Effects on Ground Reflections and Clouds.. *J. Geophys. Res.* **92**, 9740-9752

Ng, N. L., et al., 2007: Effect of NOx level on secondary organic aerosol (SOA) formation from the photooxidation of terpenes, *Atmos. Chem. Phys*. **7**, 5159–5174.

Pugh, T. A. M., Ryder J., MacKenzie, A. R., Moller, S. J., Lee, J. D., Helfter C., Nemitz E., Lowe D., Hewitt C. N., 2010: Modelling chemistry in the nocturnal boundary layer above tropical rainforest and a generalized effective nocturnal ozone deposition velocity for sub-ppbv NOx conditions, *J Atmos. Chem.* **65**, 89–110, DOI 10.1007/s10874-011-9183-4

Rohrer F., Brüning D., Grobler E. S., Weber M. Ehhalt D. H. Neubert, R. Schüßler W. Levin I., 1998: Mixing Ratios and Photostationary State of NO and NO_2 Observed During the POPCORN Field Campaign at a Rural Site in Germany, *J Atmos. Chem* **31**, 119–137.

Sander, S.P., Abbatt, J.P.D., Barker, J.R., Burkholder, J.B., Friedl, R.R., Golden, D.M., Huie, R.E., Kolb, C.E., Kurylo, M.J.., Moortgat, G.K., Orkin, V.L., Wine, P.H., 2011: Chemical Kinetics and Photochemical Data for Use in Atmospheric Studies, Evaluation No. 17; Jet Propulsion Laboratory: Pasadena, CA.

Schrimpf, W., Lienaers, K., Muller, K.P., Rudolph, J., Neubert, R., Schüßler, W., Levin, I., 1996: Dry Deposition of peroxyacetyl nitrate (PAN): Determination of its deposition velocity at night from measurements of the atmospheric PAN and ^{222}Radon concentration gradient, *Geophys. Res. Lett.* **23**, 3599-3602.

Seefeld, S., 1997. Laboratory kinetic and atmospheric modelling studies of the role of peroxyacyl nitrates in tropospheric photooxidant formation. Ph.D. Thesis, Swiss Federal Institute of Technology, Zürich, Switzerland.

Simpson, I. J., Blake N. J., Barletta B., Diskin G. S., Fuelberg H. E., Gorham K., Huey L. G., Meinardi S., Rowland F. S., Vay S. A., Weinheimer A. J., Yang M., and Blake D. R., 2010: Characterization of trace gases measured over Alberta oil sands mining operations: 76 speciated C_2–C_{10} volatile organic compounds (VOCs), CO_2, CH_4, CO, NO, NO_2, NO_y, O_3 and SO_2, *Atmos. Chem. Phys*. **10**, 11931–11954.

Singh, H. B., et al. "Pollution influences on atmospheric composition and chemistry at high northern latitudes: Boreal and California forest fire emissions." Atmospheric Environment 44.36 (2010): 4553-4564.

Stanley, Wei Yang Brian L. Jennison, and T. Omaye. "Air pollution and asthma emergency room visits in Reno, Nevada." Inhalation toxicology 9.1 (1997): 15-30.

Stelson A.W., Seinfeld J.H., 1982: Relative humidity and temperature dependence of the ammonium nitrate dissociation constant, *Atmos. Environ. 1967* **16** (5), 983-992. (http://www.sciencedirect.com/science/article/pii/0004698182901846)

Stone, D., Evans, M. J., Walker, H., Ingham, T., Vaughan, S., Ouyang, B., ... & Heard, D. E. (2014). Radical chemistry at night: comparisons between observed and modelled HOx, NO_3 and N_2O_5 during the RONOCO project. *Atmospheric Chemistry and Physics*, **14**(3), 1299-1321.

Wahner, Andreas, Thomas F. Mentel, and Martin Sohn. "Gas□phase reaction of N2O5 with water vapor: Importance of heterogeneous hydrolysis of N2O5 and surface desorption of HNO3 in a large Teflon chamber." Geophysical Research Letters 25.12 (1998): 2169-2172.

Washoe County (2014). Washoe County, Nevada air quality trends (2004-2013). prepared by Washoe County Health District, Air Quality Management Division, Reno, NV, http://www.washoecounty.us/repository/files/4/AQ-Trends-2004-13.pdf.

492 **Tables**

493 **Table 1.** Instrumentation of ancillary species for field studies.

Pollutant	Symbol	Manufacturer & model	Detection Limit	Principle of Operation
Ozone	O_3	Dasibi 1008-AH and DOAS	2 ppb	U.V. photometric and light absorption
Nitric oxide	NO	TEII 42S	0.2 ppb	Chemiluminescence
Total nitrogen oxides	NO_y	TEII 42 + ext. Mo converter	0. 2 ppb	Chemiluminescence
Nitrogen Dioxide	NO_2	DOAS* and TEII 42S	0.1 ppb	Light absorption
Nitrate radical	NO_3	DOAS*	5 ppt	Light absorption
Total nitrate	NO_3-	TEII 42 + ext. Mo converter	0.2 ppb	Chemiluminescence, the measurement used another NOy monitor with a nylon filter upstream, and NO_3- was calculated from the difference between the two instruments.
Total sulfate	SO_4--	TEI Model 5020 SPA (Sulfate Particulate Analyzer)	0.50 $\mu g/m^3$ (15 minute cycle)	Converts SO_4 to SO_2 using a thermal reduction technique. SO_2 is then analyzed using pulsed fluorescence spectroscopy. The result is a continuous analyzer producing data points every 10 seconds
Formaldehyde	HCHO	DNPH and DOAS*	50 ppt	Extraction from DNPH followed by IC, and light absorption
Carbon monoxide	CO	Aero-Laser Model AL5002	2 ppb	vacuum UV fluorescence, instrument with 1 s response time
Sulfur dioxide	SO_2	TEII 43S	0.1 ppb	pulsed fluorescence
Volatile Organic Compounds	VOC	Varian Saturn 2000 mass spectrometer, Varian 3800 GC, and Entech 7100	0.01 - 0.05 ppbv	Canisters analyzed by GC/FID/MS
Aldehydes	RCHO	Waters 2695 Alliance Separation Module	0.1 ppbv	DNPH (2,4-dinitrophenylhydrazine) cartridges
Particle size distribution and number density	0.1-10 μm	SMPS: 3080N Electrostatic Classifier and CPC 3025 Condensation Particle Counter (TSI)	2×10^2 to 5×10^7 part./cm^3 in number concentration for monodisperse 50 nm particles)	electrical-mobility particle size classification, combined with a Condensation Particle Counter (CPC)

494 * DOAS sensitivity based on a light path of at least 5 km.

Table 2. Meteorological instrumentation for field studies.

Meteorological variable	Symbol	Manufacturer & model	Sensitivity	Principle of Operation
Wind direction	WDD	MET-ONE 24A	5°	Wind vane
Wind speed	WDS	MET-ONE 21A	0.5 m/s	3-cup anemometer
Temperature	T	MET-ONE 60A	0.5°C	Thermistor
Relative humidity	RH	MET-ONE 83A	3%	Capacitance
Barometric pressure	Press	MKS-Baratron	0.2 torr	Transducer

Table 3. Range and average values of nighttime NO, NO_2, NO_3 and O_3 throughout the campaign.

Compound	Range	Average
NO	0.004 – 3.9 ppb	0.71 ppb
NO_2	0.45 – 35 ppb	3.6 ppb
NO_3	0 – 150 ppt	11 ppt
O_3	17 – 85 ppb	51 ppb

Table 4. The relative importance of NO_3 reactions compared to HO and O_3.

Date	Model Species	NO_3	HO	O_3
July 10-11	OLI	36%	3.5%	60%
(wildfire event)	DIEN	16%	59%	25%
	ISO	44%	36%	21%
	API	71%	3%	25%
July 30-31	OLI	49%	10%	42%
(Typical night)	DIEN	11%	80%	9%
	ISO	34%	57%	8%
	API	79%	7%	14%

Figures

Figure 1 Schematic of DOAS setup. The DOAS is located at DRI, with reflectors located on the hotel roof.

Figure 2 Time series for measured (a) CO, (b) acetone, and (c) aldehydes, with periods of elevated concentrations associated with the wildfire event

Figure 3 Ozone and CO concentrations during the night and early morning of July 13-14, 2008

Figure 4 Summary of NO_3 measurements throughout campaign. The average mixing ratio is depicted by blue diamonds, with the error bars showing the standard deviation of the mean.

Figure 5 Comparison of particle size distribution for a night impacted by (a) wildfires and (b) a typical night

Figure 6 Comparison of the nights of July 10-11, 2008 and July 30-31, 2008 for (a) ozone, (b) NO_2, (c) NO, and (d) NO_3 including measurements and 0-D model output

Figure 7 Model predictions for HO concentrations for the nights of July 10-11 and July 30-31, 2008

Figure 8 Model predictions for HO_2 concentrations for the nights of July 10-11 and July 30-31, 2008

Figure 9 Total HOx (HO + HO_2) formation rates during the nights of July 10-11 (polluted night) and July 30-31 (typical night) in Reno, NV

Figure 10 Modeled HO_2/HO Ratios for July 10-11 and July 30-31

Figure 11 Relative removal rates of NO_3 by hydrocarbons for (a) July 10-11, and (b) July 30-31, 2008

Figure 12 Relative rates of nitric acid formation on (a) July 10-11, 2008 and (b) July 30-31, 2008 in Reno, NV

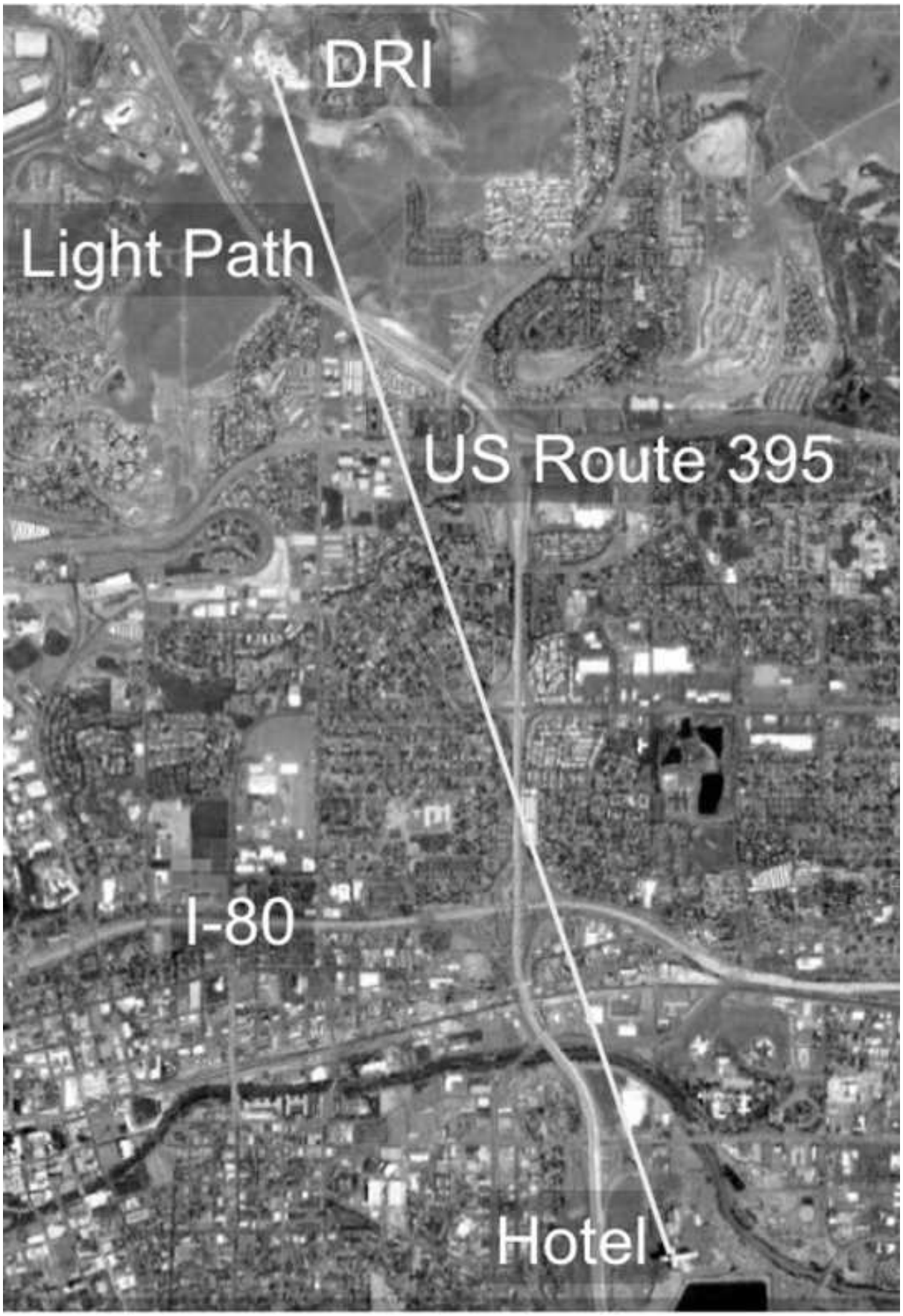
DRI
Light Path
US Route 395
I-80
Hotel

(a)

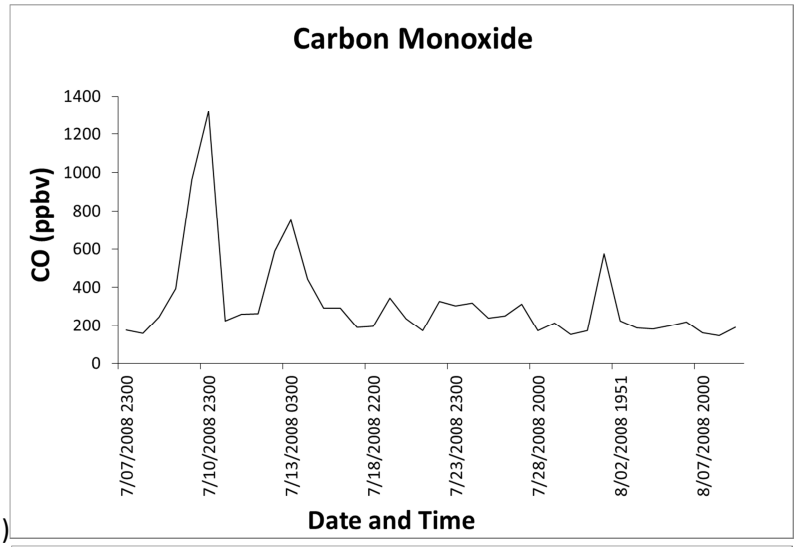
Carbon Monoxide
CO (ppbv)
1400
1200
1000
800
600
400
200
0
7/07/2008 2300
7/10/2008 2300
7/13/2008 0300
7/18/2008 2200
7/23/2008 2300
7/28/2008 2000
8/02/2008 1951
8/07/2008 2000
Date and Time

(b)

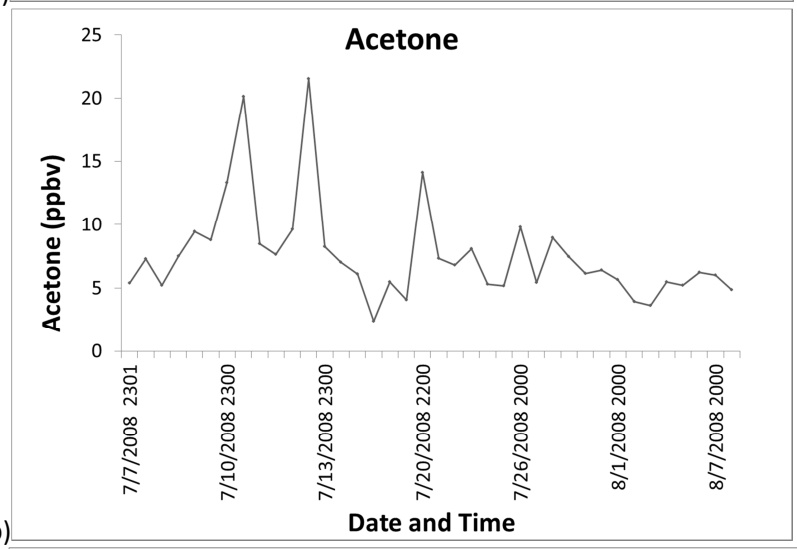
Acetone
Acetone (ppbv)
25
20
15
10
5
0
7/7/2008 2301
7/10/2008 2300
7/13/2008 2300
7/20/2008 2200
7/26/2008 2000
8/1/2008 2000
8/7/2008 2000
Date and Time

(c)

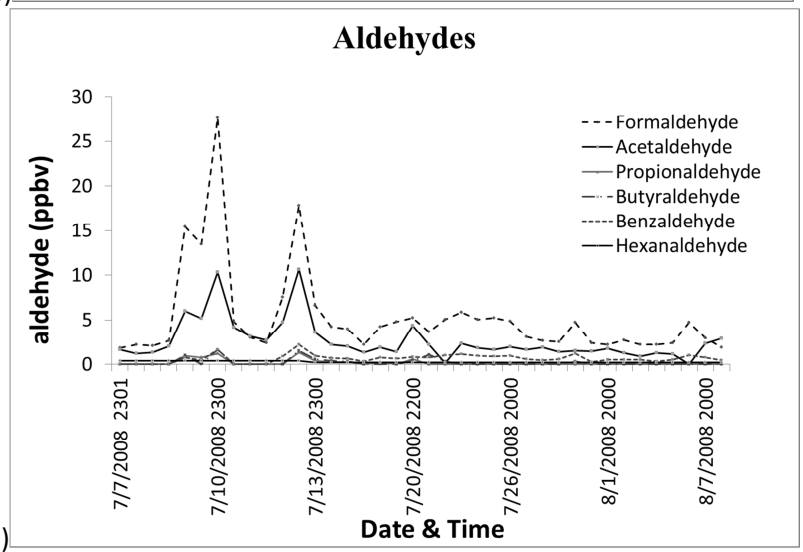
Aldehydes
aldehyde (ppbv)
30
25
20
15
10
5
0
Formaldehyde
Acetaldehyde
Propionaldehyde
Butyraldehyde
Benzaldehyde
Hexanaldehyde
7/7/2008 2301
7/10/2008 2300
7/13/2008 2300
7/20/2008 2200
7/26/2008 2000
8/1/2008 2000
8/7/2008 2000
Date & Time

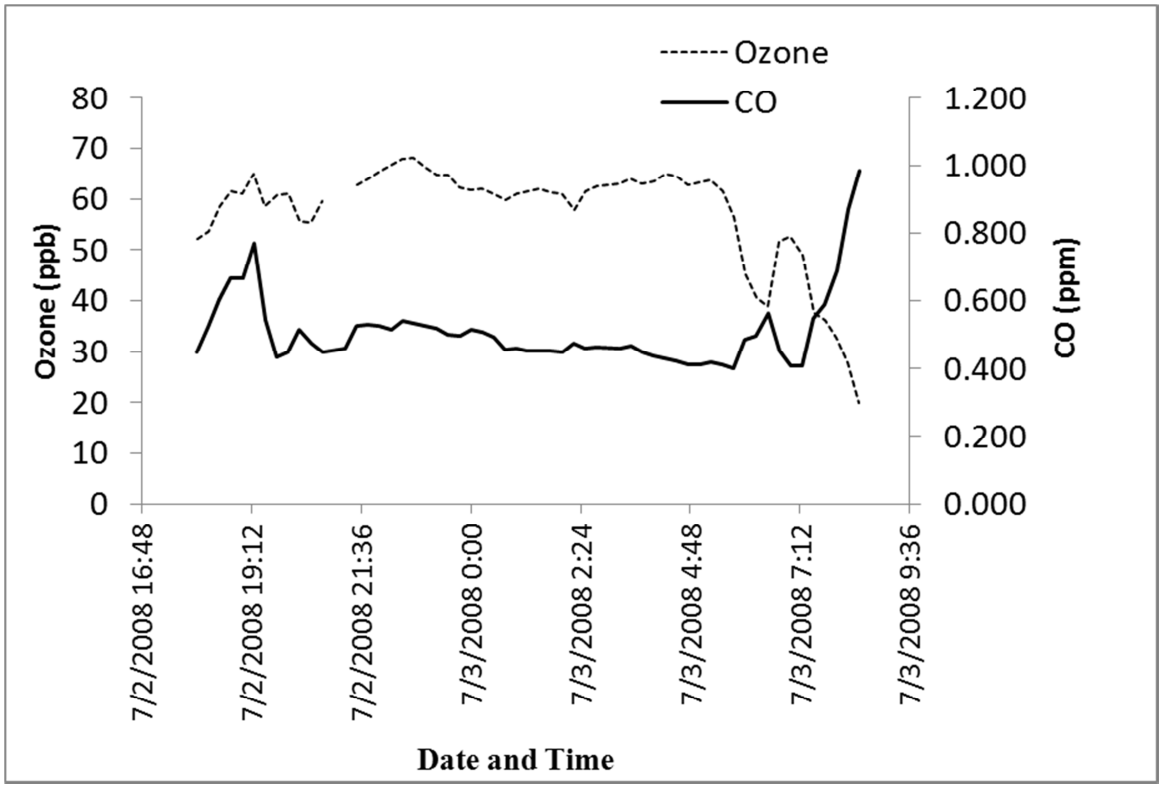
Ozone
CO
80
70
60
50
40
30
20
10
0
Ozone (ppb)
1.200
1.000
0.800
0.600
0.400
0.200
0.000
CO (ppm)
7/2/2008 16:48
7/2/2008 19:12
7/2/2008 21:36
7/3/2008 0:00
7/3/2008 2:24
7/3/2008 4:48
7/3/2008 7:12
7/3/2008 9:36
Date and Time

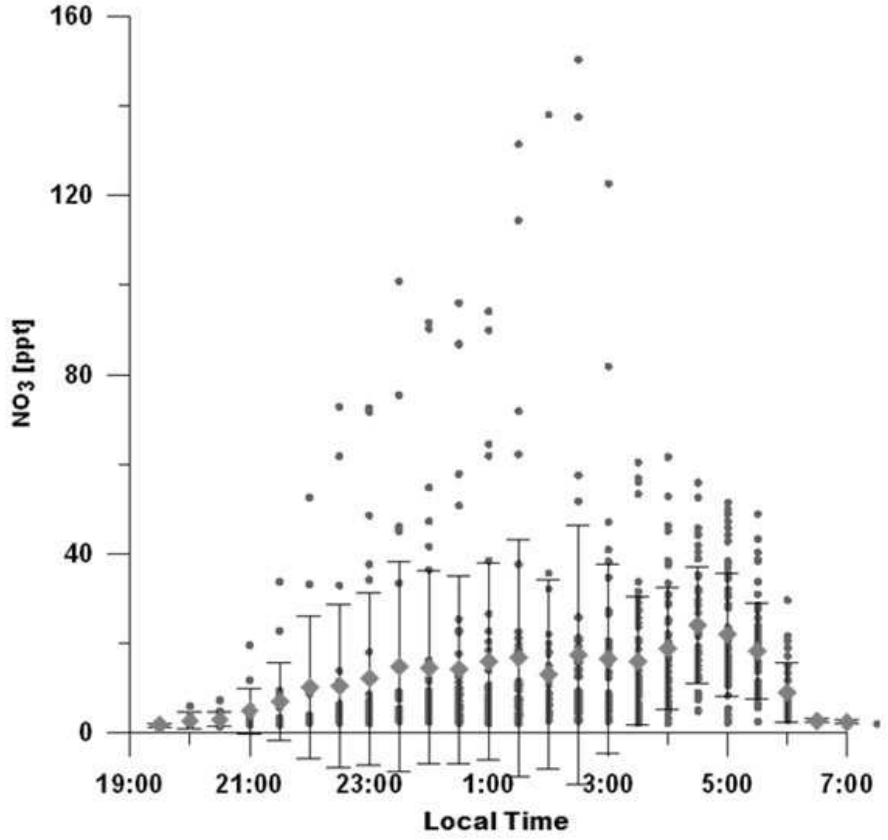
160
120
80
40
0
NO3 [ppt]
19:00
21:00
23:00
1:00
3:00
5:00
7:00
Local Time

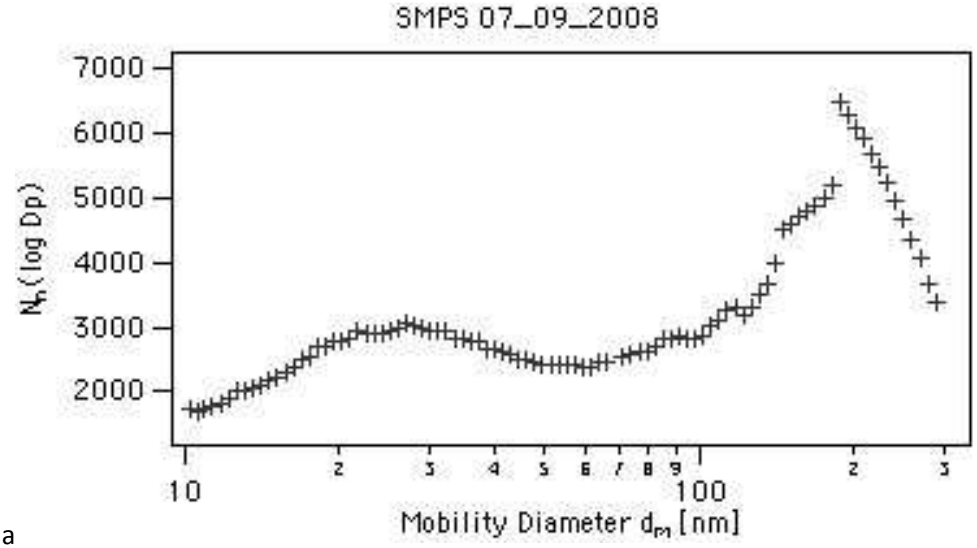
SMPS 07_09_2008
7000
6000
5000
4000
3000
2000
N (log Dp)
10
100
Mobility Diameter d [nm]

a

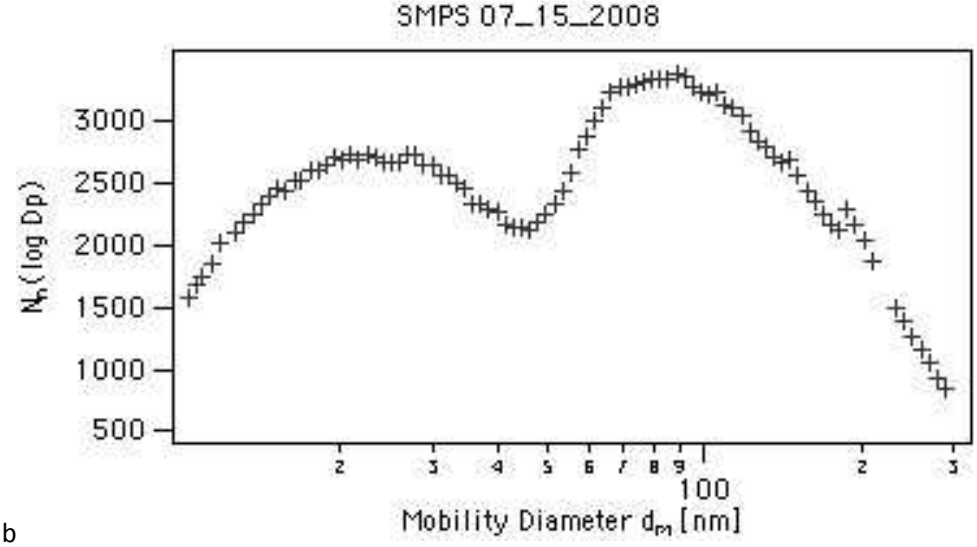
SMPS 07_15_2008
3000
2500
2000
1500
1000
500
N (log Dp)
100
Mobility Diameter d [nm]

b

(a)

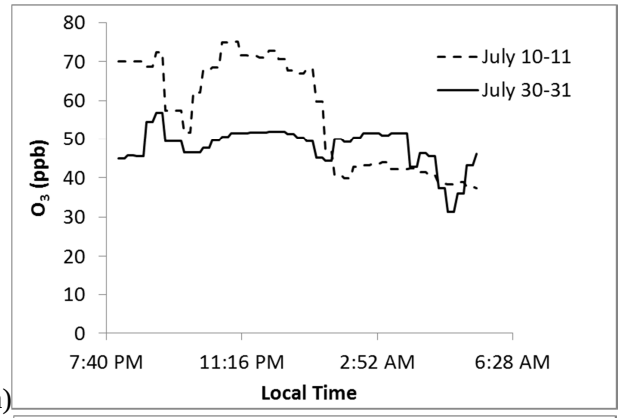
80
70
60
50
40
30
20
10
0
O_3 (ppb)
July 10-11
July 30-31
7:40 PM
11:16 PM
2:52 AM
6:28 AM
Local Time

(b)

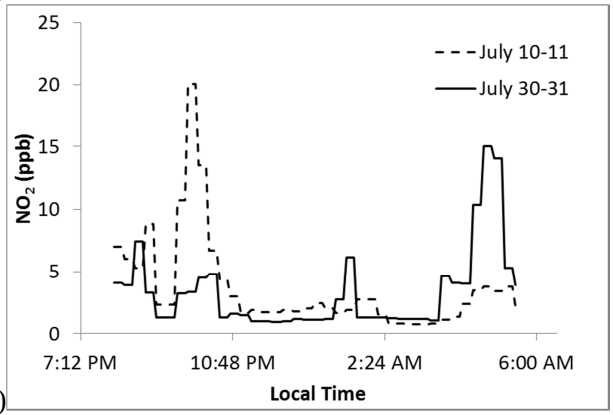
25
20
15
10
5
0
NO_2 (ppb)
July 10-11
July 30-31
7:12 PM
10:48 PM
2:24 AM
6:00 AM
Local Time

(c)

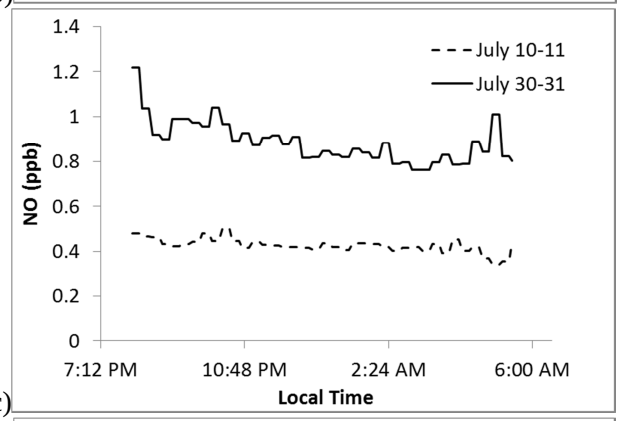
1.4
1.2
1
0.8
0.6
0.4
0.2
0
NO (ppb)
July 10-11
July 30-31
7:12 PM
10:48 PM
2:24 AM
6:00 AM
Local Time

(d)

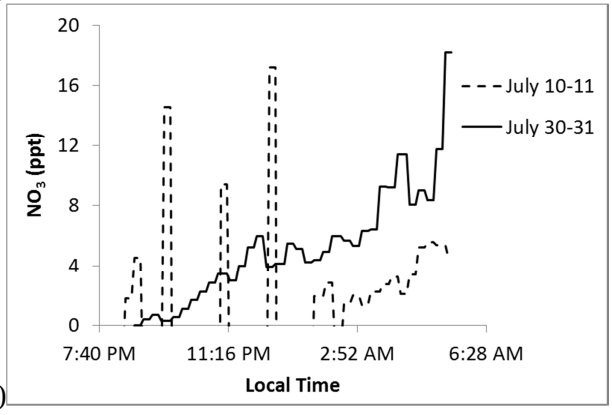
20
16
12
8
4
0
NO_3 (ppt)
July 10-11
July 30-31
7:40 PM
11:16 PM
2:52 AM
6:28 AM
Local Time

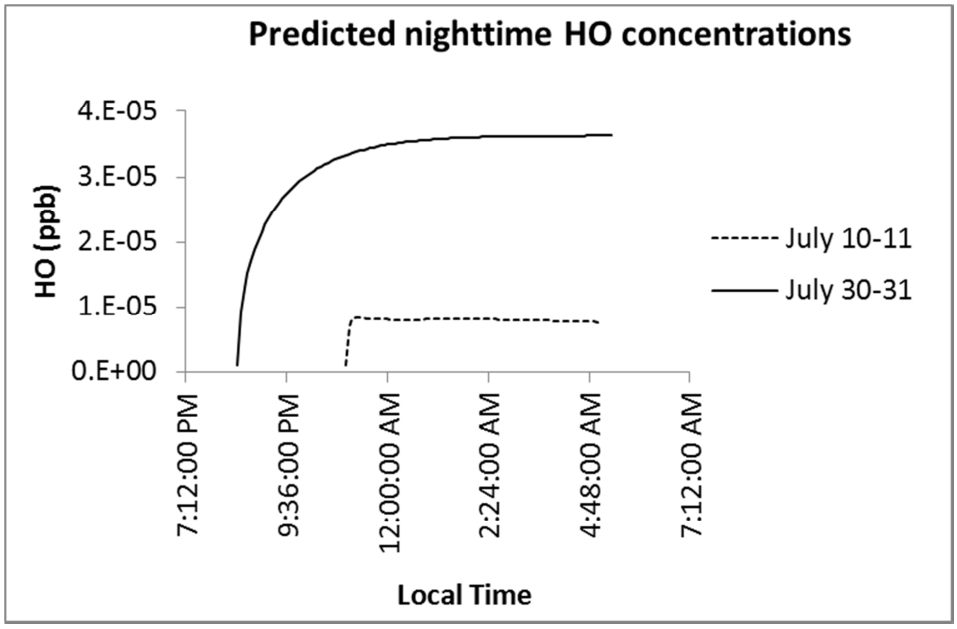
Predicted nighttime HO concentrations
HO (ppb)
4.E-05
3.E-05
2.E-05
1.E-05
0.E+00
7:12:00 PM
9:36:00 PM
12:00:00 AM
2:24:00 AM
4:48:00 AM
7:12:00 AM
Local Time
July 10-11
July 30-31

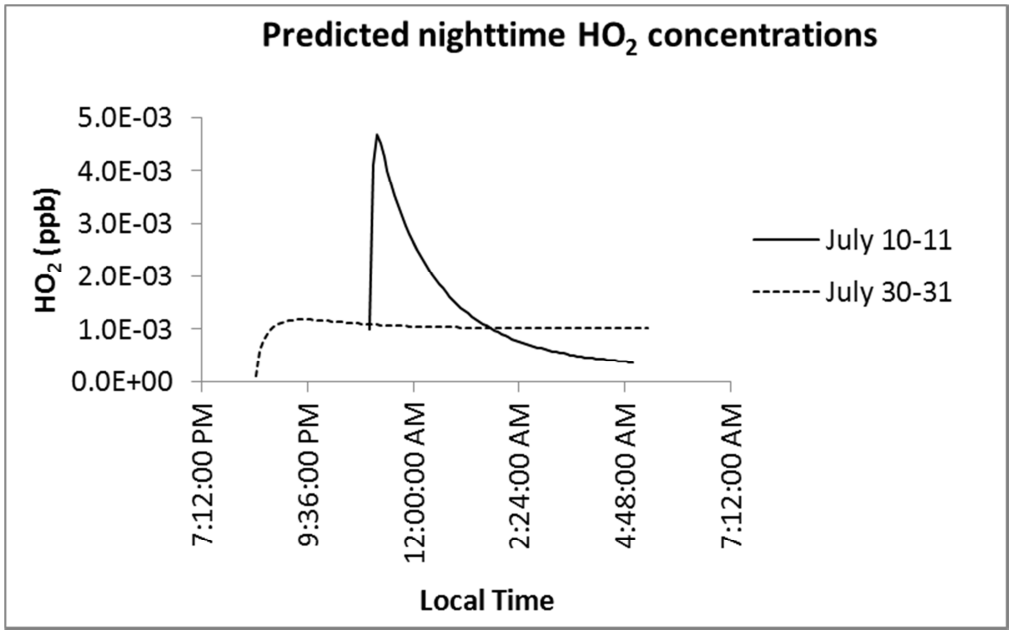
Predicted nighttime HO2 concentrations
5.0E-03
4.0E-03
3.0E-03
2.0E-03
1.0E-03
0.0E+00
HO2 (ppb)
7:12:00 PM
9:36:00 PM
12:00:00 AM
2:24:00 AM
4:48:00 AM
7:12:00 AM
Local Time
July 10-11
July 30-31

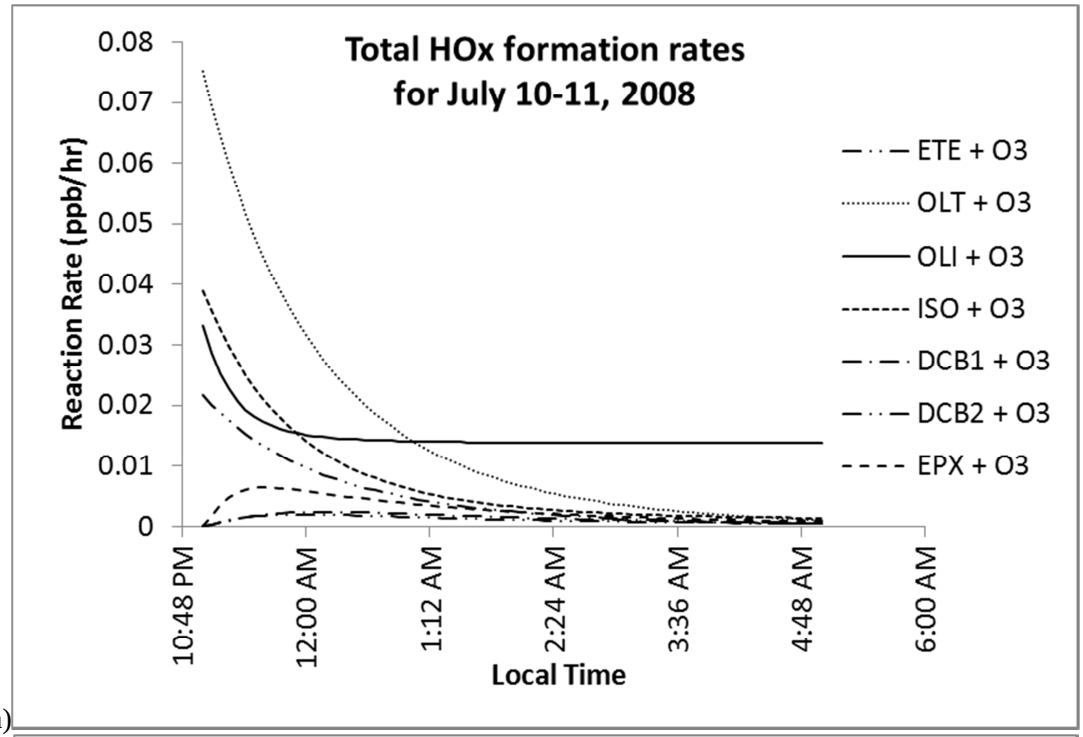
Total HOx formation rates
for July 10-11, 2008
Reaction Rate (ppb/hr)
0.08
0.07
0.06
0.05
0.04
0.03
0.02
0.01
0
10:48 PM
12:00 AM
1:12 AM
2:24 AM
3:36 AM
4:48 AM
6:00 AM
Local Time
ETE + O3
OLT + O3
OLI + O3
ISO + O3
DCB1 + O3
DCB2 + O3
EPX + O3

(a)

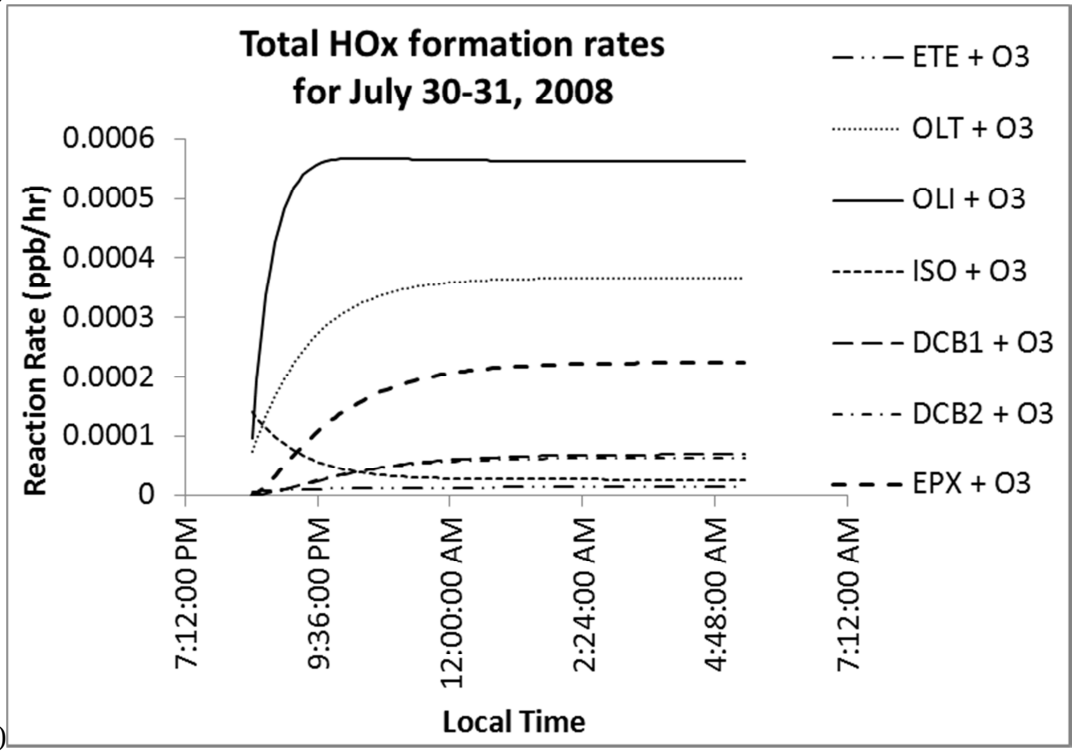
Total HOx formation rates
for July 30-31, 2008
Reaction Rate (ppb/hr)
0.0006
0.0005
0.0004
0.0003
0.0002
0.0001
0
7:12:00 PM
9:36:00 PM
12:00:00 AM
2:24:00 AM
4:48:00 AM
7:12:00 AM
Local Time
ETE + O3
OLT + O3
OLI + O3
ISO + O3
DCB1 + O3
DCB2 + O3
EPX + O3

(b)

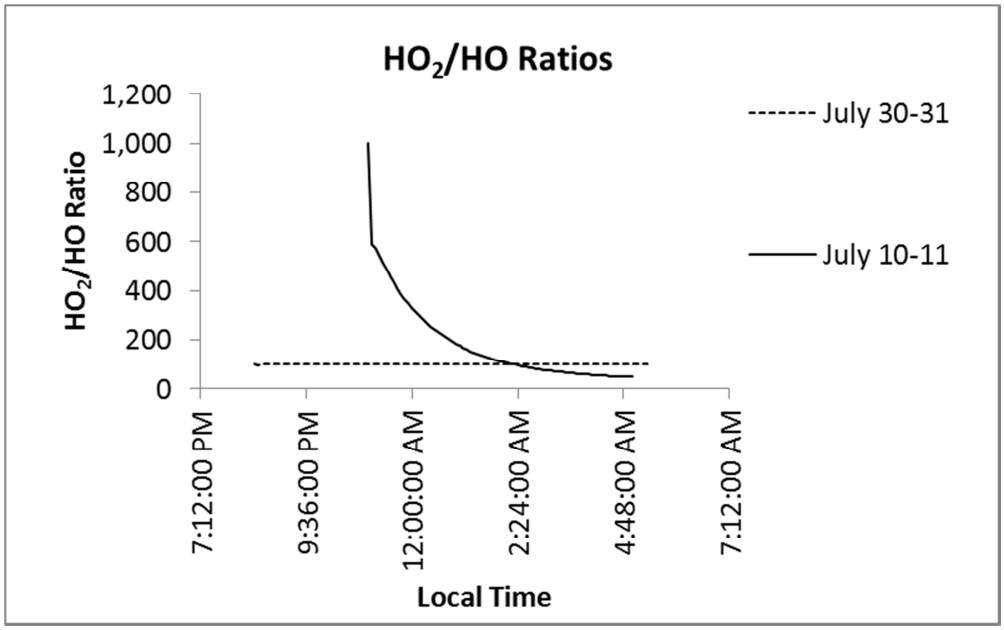
HO2/HO Ratios
HO2/HO Ratio
1,200
1,000
800
600
400
200
0
7:12:00 PM
9:36:00 PM
12:00:00 AM
2:24:00 AM
4:48:00 AM
7:12:00 AM
Local Time
July 30-31
July 10-11

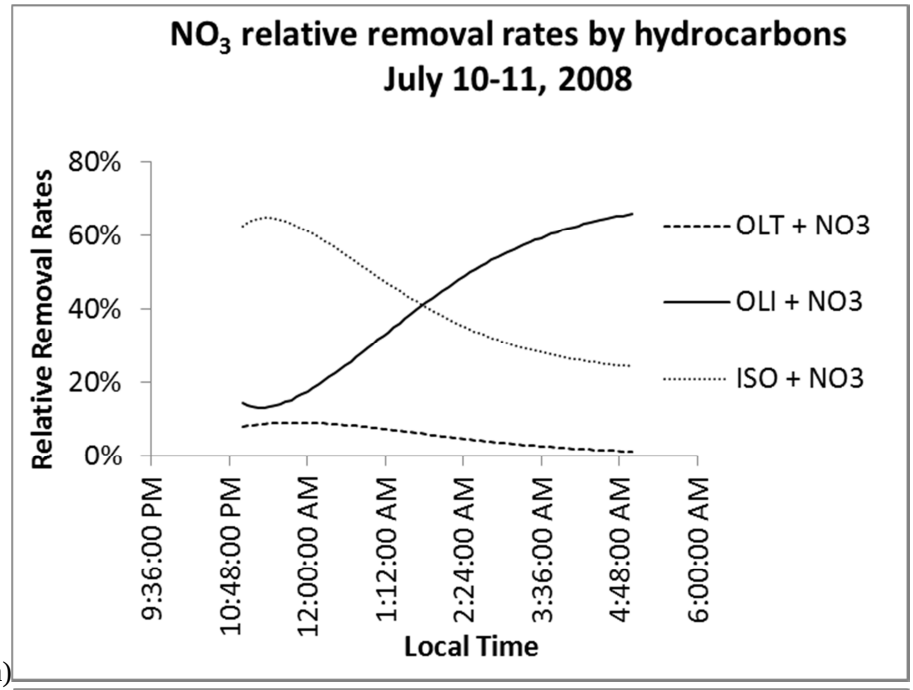
NO3 relative removal rates by hydrocarbons
July 10-11, 2008
Relative Removal Rates
80%
60%
40%
20%
0%
9:36:00 PM
10:48:00 PM
12:00:00 AM
1:12:00 AM
2:24:00 AM
3:36:00 AM
4:48:00 AM
6:00:00 AM
Local Time
OLT + NO3
OLI + NO3
ISO + NO3

(a)

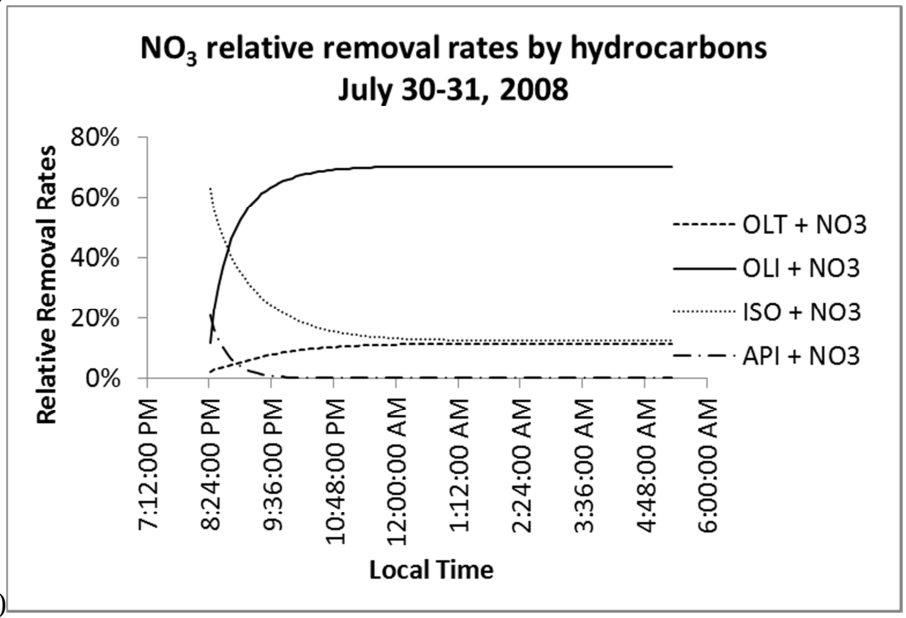
NO3 relative removal rates by hydrocarbons
July 30-31, 2008
Relative Removal Rates
80%
60%
40%
20%
0%
7:12:00 PM
8:24:00 PM
9:36:00 PM
10:48:00 PM
12:00:00 AM
1:12:00 AM
2:24:00 AM
3:36:00 AM
4:48:00 AM
6:00:00 AM
Local Time
OLT + NO3
OLI + NO3
ISO + NO3
API + NO3

(b)

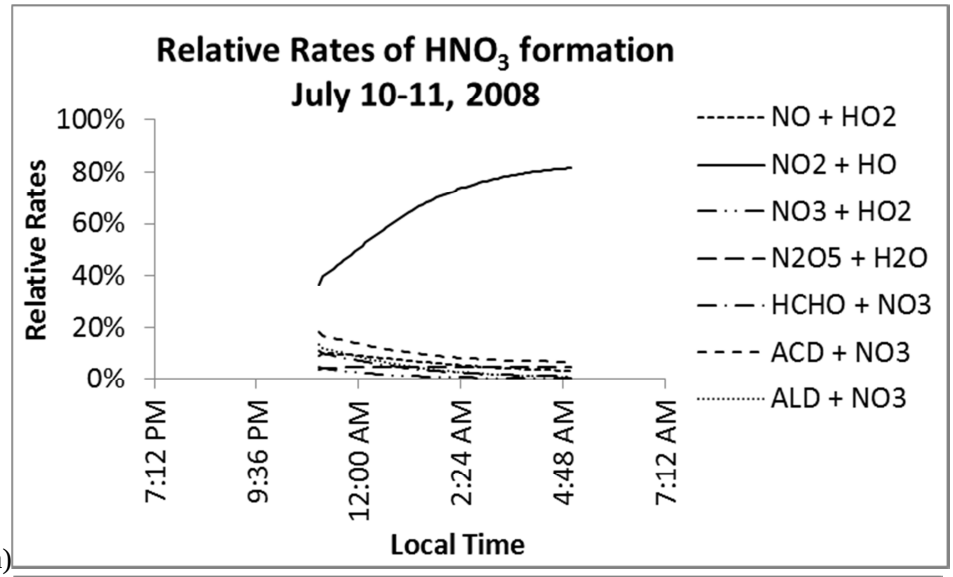
Relative Rates of HNO3 formation
July 10-11, 2008
Relative Rates
100%
80%
60%
40%
20%
0%
7:12 PM
9:36 PM
12:00 AM
2:24 AM
4:48 AM
7:12 AM
Local Time
NO + HO2
NO2 + HO
NO3 + HO2
N2O5 + H2O
HCHO + NO3
ACD + NO3
ALD + NO3

(a)

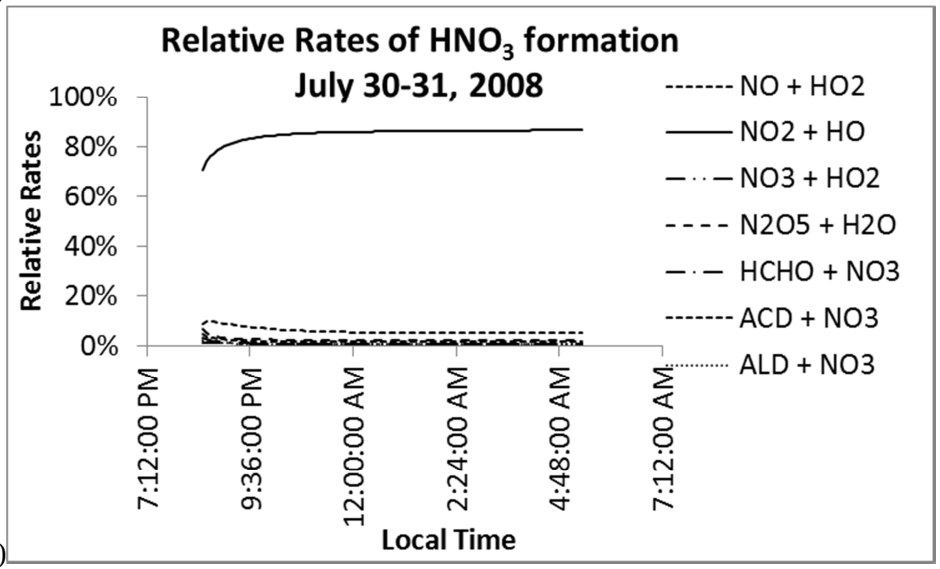
Relative Rates of HNO3 formation
July 30-31, 2008
Relative Rates
100%
80%
60%
40%
20%
0%
7:12:00 PM
9:36:00 PM
12:00:00 AM
2:24:00 AM
4:48:00 AM
7:12:00 AM
Local Time
NO + HO2
NO2 + HO
NO3 + HO2
N2O5 + H2O
HCHO + NO3
ACD + NO3
ALD + NO3

(b)